

Density Functional Studies of 2-(4-bromophenyl)-2-(4-fluorophenylamino) acetonitrile

Sanjeev Kumar Trivedi

Department of Physics, Mumtaz P. G. College, University of Lucknow, Lucknow-226007, India

Abstract: We have performed extensive theoretical calculations to investigate the structural and vibrational properties of 2-(4-bromophenyl)-2-(4-fluorophenylamino)acetonitrile (**1**). The molecular geometry, harmonic vibrational frequencies and bonding features of the molecule **1** at the ground state have been studied. The assignment of the fundamental vibrations modes have been done on the basis of the potential energy distribution (PED).

Keywords: Alpha-aminonitrile, Vibrational Analysis, FTIR, Molecular Orbital

1. Introduction

Alpha-aminonitriles are the versatile precursors of a wide range of pharmaceutically relevant natural and unnatural molecules of interest; they are the key precursors of diverse α -amino-acids finding applications in synthesizing proteins and also as chiral building blocks in the pharmaceutical industry. Alpha-aminonitriles constitute key parts of several pharmaceutically important bioactive molecules such as clopidogrel, prasugrel, saframycin A, manzacidin A-C, ecteinascidin 743, and phtalascidin [1, 2]. Furthermore, they are also regarded as versatile intermediates for the preparation of 1, 2-diamines, and nitrogen or sulfur-containing heterocycles such as imidazoles and thiadiazoles [1].

2. Results and discussion

All quantum chemical calculations of the title compound are carried out with Gaussian 09 suite of program [3] using the

B3LYP/6-311+G (d,p) levels of theory to predict the molecular structure and vibrational wave numbers.

2.1 Molecular Structure and Optimized Geometry

The optimized geometry for ground state lower energy conformer is shown in **Figure 2**. The selected optimized parameters of the title compound calculated at B3LYP/6-311+ G (d, p), are listed in the **Table 1**. The molecule possesses C_1 symmetry. The bond length, bond angle and dihedral angles are calculated for the equilibrium state of the alpha-aminonitrile molecule **1**.

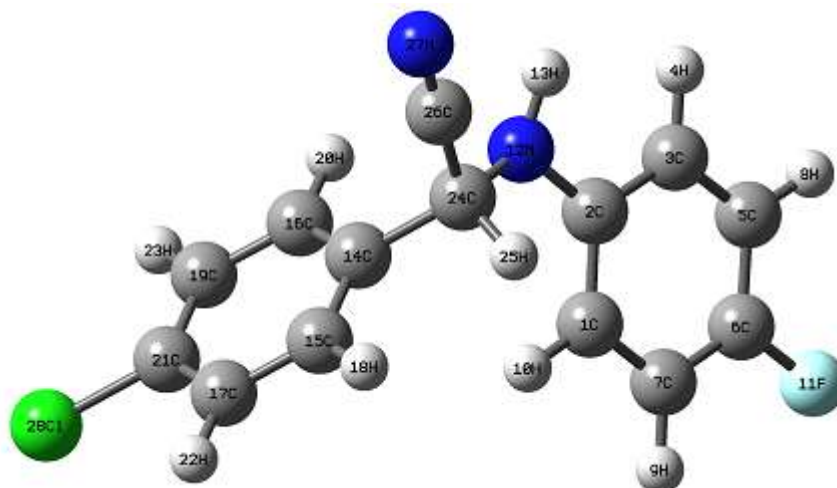


Figure 2: Optimized structure of alpha-aminonitrile **1**

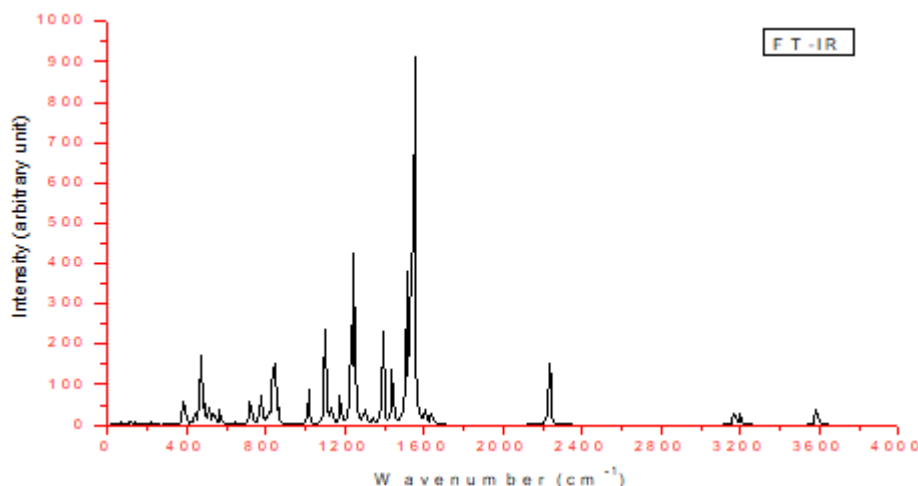


Figure 2: Cal. IR plot of the title compound,

Table 1: Selected bond lengths (angstroms), bond angles (degrees) calculated at the B3LYP/+31-6G(d,p) level.

Parameter	Calculated	Parameter	Calculated	Parameter	Calculated
C1-C2	1.39	C1-C6	1.39	C1-H27	1.76
C2-C3	1.39	C2-N7	1.09	C3-C4	1.39
C3-N8	1.09	C4-C5	1.39	C4-C11	1.54
C5-C6	1.39	C5-H9	1.09	C6-H10	1.09
C11-H12	1.43	C11-N13	1.48	C12-N26	1.26
N13-H14	1.01	N13-C15	1.37	C15-C16	1.39
C15-C20	1.39	C16-C17	1.39	C16-H21	1.09
C17-C18	1.39	C17-H22	1.09	C18-C19	1.39
C18-H25	1.35	C19-C20	1.39	C19-C23	1.09
C20-H24	1.09	C2-C1-C6	120.0	C2-C1-C127	120.0
C6-C1-C127	120.0	C1-C2-C3	120.0	C1-C2-H7	119.9
C3-C2-H7	120.0	C2-C3-C4	119.9	C2-C3-H8	120.0
C4-C3-H8	119.9	C3-C4-C5	119.9	C3-C4-C11	119.9
C5-C4-C11	120.0	C4-C5-C6	120.0	C4-C5-H9	120.0
C6-C5-H9	119.9	C1-C6-C5	120.0	C1-C6-H10	120.0
C5-C6-H10	119.9	C4-C11-C12	117.8	C12-C11-N13	114.0
C11-N13-H14	110.8	C11-N13-C15	130.9	H14-N13-C15	118.2
N13-C15-C16	122.7	N13-C15-C20	117.2	C16-C15-C20	120.0

2.2 Vibrational Analysis

The selected theoretical and experimental vibrational modes of the title molecule, calculated using B3LYP/6-311+ G(d, p) method and their assignments using PED (Potential Energy Distribution) are given in Table 2. The vibrational band assignments have been done on the basis of normal co-ordinate analysis.. The maximum number of potentially

active observable fundamentals of a nonlinear molecule which contains N atoms is equal to (3N-6) modes of vibrations [6, 7]. The molecule consists of 27 atoms hence undergoes 75 normal modes of vibration. The experimental and calculated frequencies and their assignment are presented in Table 2.

Table 2: Vibrational analysis of prominent modes of acetonitrile at the B3LYP/6-311++G(d,p) level

Frequency (cm ⁻¹)	Intensity	FTIR		
Calc.	Scaled	I.R	Freq.	Assignment
				(<10%)
3607	3486	28.66	3351	ν_{as} (N12-H13)(100)
3205	3098	0.88	3125	R[ν_{as} (C7-H9)(42) + ν (C1-H10)(57)]
3205	3097	1.12	—	R[ν (C16-H20)(32) + ν (C19-H23) (61)]
3202	3094	1.25	—	R[ν (C17-H22)(85)]
3200	3093	1.98	—	R[ν (C5-H8)(85)]
3192	3085	7.05	—	R[ν (C16-H20) + ν (C19-H23) (85)]
3164	3057	8.47	—	R[ν (C3-H4)(37) + ν (C5-H8)(16)]
3162	3056	5.15	2938	R[ν (C15-H18)(85)]
2349	2270	7.05	2250	R[ν_{as} (N27-C26)(91)]
1654	1598	0.19	—	R[ν_{as} (C3-C5)(53) + (H4-C3-C5)(18)]
1639	1584	8.47	—	R[ν (C1-C2)(15) + (C6-C7)(20) + (C5-C6) (21)]
1632	1577	5.15	1625	R[ν_{as} (C17-C15)(50) + ν_{as} (C19-C16)(12)]
1542	1490	8.02	1509	R[σ (H4-C3-C5)(46)]
1526	1475	7.99	1487	R[ν (C3-C5)(16) + (H13-N12-C2) (47)]
1517	1466	2.15	—	R[ν (C14-C16)(18) + (H18-C15-C17)(14)]
1435	1387	20.04	—	R[ν (C3-C5)(18) + σ (H-N7-C9)(13)]
1432	1384	7.16	—	R[ν (C3-C5)(47) + ρ (H4-C3-C5)(14)]
1357	1311	31.00	—	R[ν_{as} (C14-C16)(22) + (σ (H25-C24-N12)(13) (72)]
1344	1299	15.48	—	R[ν (C1-C2)(23) + σ (H9-C7-C1)(24)]
1326	1282	1.70	—	R[σ (H4-C3-C5)(80)]
1319	1275	1.02	—	R[ν (N12-C2)(18) + ω (H26-C25-C27)(32)]
1314	1270	18.27	—	R[ν_{as} (N12-C2)(18) + ω (H4-C3-C5)(32)]
1288	1245	53.08	1242	ν_{as} (C14-C16)(16) + ω (H26-C25-C27)(21)
1271	1228	8.17	1228	ν_{as} (N12-C2)(16)
1240	1198	188.05	—	R[ν (N-H10)(85) + ω (H-N7-C9)(14)]
1204	1164	5.16	—	R[ν (C1-C10)(85)]
1179	1140	13.04	—	R[σ (H-N7-C9)(14)]
1138	1100	18.25	—	R[ν (C21-C128)(85) + (H23-C19-C21)(14)]
1129	1091	10.51	—	R[σ (H4-C3-C5)(47)]
1101	1064	74.52	—	R[ν (N12-C25)(43)]
1097	1060	13.67	1097	R[ν (C21-C128)(10) + (N12-C24)(37)]
1030	995	34.41	—	R[σ (C-C-C10)(85) + σ (C-C7-C9)(14)]
1024	990	2.12	1017	ν (N12-C25)(43)]
997	964	2.00	—	ν (C24-C25)(29)
987	954	0.81	—	R[τ (H18-C15-C17-N21)(85)]
963	930	0.41	—	R[τ (C-C-C10)(85) + τ (C-C7-C9)(14)]
952	920	0.03	—	R[τ (H-C-C-N10)(85)]
870	841	0.72	834	R[ν (C7-C9)(14)]
854	826	32.58	826	R[ν (C7-C9)(14)]
737	712	3.35	699	R[τ (C1-C2-N12-C25)(19)]
701	677	3.6	655	R[σ (C-C7-C9-C)(14)]
542	524	11.85	513	R[τ (C128-C21-C19-C10)(11)]
497	480	5.23	484	R[τ (H-N7-C9-C)(14)]

Abbreviations used here have following meaning: ν_{as} ; asymmetric stretching, ν ; symmetric stretching, σ ; scissoring, ρ ; rocking, τ_o ; out of plane torsion, τ_i ; in the plane torsion, R ; carbon ring.

2.2.1 N-H vibration

The N-H stretching of the title compound is observed at 3351 cm⁻¹, whereas this is calculated as 3408cm⁻¹. As expected, this is a pure stretching mode and also evident by its PEd, i.e. 100% . The weak band of N-H scissoring vibration is calculated at 1607 cm⁻¹ and 537 cm⁻¹ which represent the N-H scissoring and torsion mode of vibrations, respectively.

2.2.2 C-H vibration

The aromatic structure of the title compound **1** shows the presence of C-H stretching vibration in the region 3077-3040 cm⁻¹, which is also the characteristic region for the identification of C-H stretching vibration [12, 13] and is assigned well with the peak in the region 2847- 3065 cm⁻¹ in FTIR spectra. These vibrations are not found to be affected due to the nature and position of the substituent.

Rocking mode of methylene vibration is calculated to be 1306 cm⁻¹.

The C-H in plane bending frequencies for the alpha-aminonitrile appear in the range 1287-1018 cm⁻¹ and are very useful for the characterization purpose [14]. The C-H in plane bending vibration appear as strong bands in the FTIR spectrum at 1192, 1130, 1128 cm⁻¹ and 1116, 1018 cm⁻¹ in FTIR spectrum. The C-H out of plane bending vibrations are strongly coupled vibrations occurring in the region 1000-750 cm⁻¹ [15] and corresponding FTIR spectra observed at 937 cm⁻¹ and 833 cm⁻¹.

2.2.3 C-C vibration

In aromatic hydrocarbon, skeletal vibrations involving carbon-carbon stretching within ring are observed in the region 1614-1524 cm⁻¹. The C-C aromatic stretching

vibrations gives rise to characteristics bands in the spectral range from 1643-1577 cm^{-1} . Therefore, the C-C stretching vibrations of alpha-aminonitrile are found in the region 1636-1142 cm^{-1} and in FTIR spectrum at 1509 cm^{-1} and 1487 cm^{-1} . Most of the ring vibrational modes are affected by the substitution in the aromatic ring of alpha-aminonitrile. Other mode of vibrations such as scissoring and torsion are found at lower frequencies.

2.2.4 C \equiv N vibration

The stretching vibration of the triply-bonded groups occurs between 2500 and 2000 cm^{-1} . The group C \equiv N gives rise to a strong absorption in the 2173 cm^{-1} . The C \equiv N stretching vibrations in the title molecule are found at 2250 cm^{-1} in the FTIR spectra. The in-plane and out of plane bending such as scissoring and torsion, C \equiv N vibrations have also been identified at lower frequencies and presented in the assignment table.

2.2.5 C-F vibration

The carbon-fluorine bond is a polar covalent bond between carbon and fluorine and is a component of all the organo-fluorine compounds. The high electro-negativity of fluorine gives the carbon fluorine bond a significant polarity and dipole moment. Assignments of the C-F stretching modes are very difficult as these vibrations are strongly coupled with the other in-plane bending vibrations of several modes. Normally the observed bands of the C-F stretching vibrations have been found in the range 1016-1235 cm^{-1} for several fluoro-benzenes. The C-F stretching modes are observed at 1008 and 1278 cm^{-1} in the case of the alpha-aminonitrile **1**.

2.3 HOMO-LUMO surfaces analysis

The frontier molecular orbital, highest occupied molecular orbitals (HOMOs) and lowest molecular orbitals (LUMOs) offer a reasonable qualitative prediction of the excitation properties and the ability of electron transport [16, 17]. The HOMO primarily acts as an electron donor and LUMO acts as an electron acceptor and are the main orbital which takes part in chemical stability [18]. The frontier molecular orbital gap has been used as a measure for the bioactivity, since the intra-molecular charge transfer determining the bioactivity depends on this energy gap. The HOMO and LUMO plots of title compound are shown in **Figure 4**.

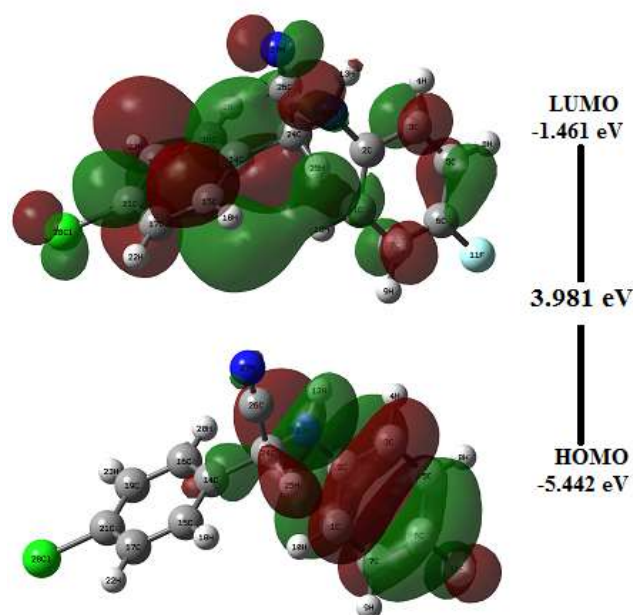


Figure 4: HOMO-LUMO Plot of the alpha-aminonitrile

The energies of HOMO and LUMO of title compound are calculated by using B3LYP/6-311++G (d, p) Method. The LUMO of title compound is delocalized over whole ring system whereas the HOMO is contributed by some molecule except fluorine attached rings. The energy gap between frontier molecular orbital of title compound is 3.98 eV.

2.4 Molecular Electrostatic Potential Surface Analysis

The potential applications of the molecular electrostatic potential (MESP) for the interpretation and prediction of chemical reactivity have been recognized. Such as the study of biological interactions, analysis of the molecular similarity, description of the crystalline state, salvation phenomena, and the topographical analysis of the electronic structure of complex molecule. The electrostatic potential sites close to the polar group is influenced by the stereo structure and the charge density distribution. Positive potential region in the studied molecules are found around the hydrogen atom of the amide group which can be considered as possible sites for nucleophilic attack. The regions close to the other polar atom chlorine are of almost zero electrostatic potential. The molecular electrostatic potential (MESP) is related to the electron density and is a very useful to understanding sites for electrophilic (negative region) and nucleophilic (positive region) reactions [17, 18]. MESP is also well suited for analyzing process based on the "recognition" of one molecule by another, as in drug receptor, and enzyme-substrate interactions, because it is through this interaction that the two entities first feel each other [19, 20]. To predict reactive sites for electrophilic and nucleophilic attack, for the investigated molecule, MESP is calculated at the B3LYP/6-311++G (d, p) and shown in **Figure 5**. The different values of the electrostatic potential at the surface are represented by different colors and potential increases in the order red<orange<yellow<green<blue. The color code of these maps is in range between -0.04315 a.u. and 0.04315 a.u. in the title compound, where blue indicates the most electropositive i.e. electron poor region and red indicates the

most electronegative region i.e. electron rich region. From the MESP it is evident that the most electropositive region is located over nitrogen bonded with hydrogen, which effectively acts as electron poor and most electronegative region is located over nitrogen, triple bonded with carbon which is electron rich region.

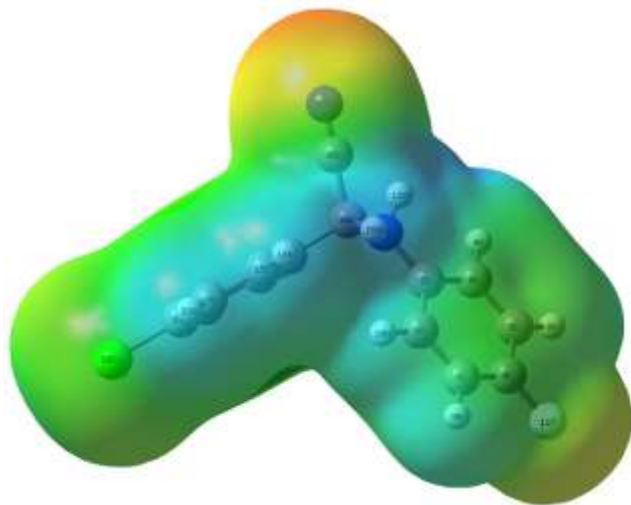


Figure 5: Molecular Electrostatic Potential Surface of the alpha-aminonitrile

3. Conclusions

In the present work, with the help of DFT calculations we have calculated the geometrical parameters, vibrational frequencies, HOMO-LUMO and MESP surfaces of a synthetic alpha-aminonitrile compound, 2-(4-bromophenyl)-2-(4-fluorophenylamino) acetonitrile (1).

References

- [1] Brahmachari, G. and Banerjee, B. (2012) *Asian J. Org. Chem.* **1**, 251-258.
- [2] Brahmachari, G., Banerjee, B., Kumar, B., Kant, R. and Gupta, V. K. (2015) *J. Indian Chem. Soc.* **92**, 1473-1478.
- [3] M.J. Frisch, G.W. Trucks, H.B. Schlegel, G.E. Scuseria, M.A. Robb, J.R. Cheeseman, G. Scalmani, V. Barone, B. Mennucci, G.A. Petersson, H. Nakatsuji, M. Caricato, X. Li, H.P. Hratchian, A.F. Iamaylov, J. Bloino, G. Zheng, J.L. Sonnenberg, M. Hada, M. Ehara, K. Toyota, R. Fukuda, J. Hasegawa, M. Ishida, T. Nakajima, Y. Honda, O. Kitao, H. Nakai, T. Vreven, J.A. Montgomery jr, J.E. Peralta, F. Ogliaro, M. Bearpark, J.J. Heyd, E. Brothers, K.N. Kudin, V.N. Staroverov, R. Kobayashi, J. Normand, K. Raghavachari, A. Rendell, J.C. Burant, S.S. Lyengar, J. Tomasi, M. Cossi, N. Rega, J.M. Millam, M. Klene, J.E. Knox, J.B. Cross, V. Bakken, C. Adamo, J. Jaramillo, R. Gomperts, R.E. Stratmann, O. Yazyev, A.J. Austin, R. Cammi, C. Pomelli, J.W. Ochterski, R.L. Martin, K. Morokuma, V.G. Zakrzewski, G.A. Voth, P. Salvador, J.J. Dannenberg, S. Dapprich, A.D. Daniels, O. Farkas, J.B. Foresman, J.V. Ortiz, J. Cioslowski, D.J. Fox, Gaussian 09, Revision A.1 Gaussian Inc., Wallingford CT, (2009).
- [4] A. D. Becke, *J. Chem. Phys.* **98** (1993) 5648-5652.

- [5] C. Lee, W. Yang, R. G. Parr, *Phys. Rev. B* **1337** (1988) 785-790.
- [6] R.M. Silverstein, G.C. Bassler, T.C. Morrill, *Spectrometric Identification of Organic Compounds*, John Wiley and sons, (1991).
- [7] G. Socrates, *Infrared and Raman characteristic Group Frequencies-Tables and Charts*, Third ed., Wiley. New York, (2001).
- [8] R. Dennington, T. Keith, J. Millam, *Gauss View*, Version 5, Semichem Inc., Shawnee Mission KS, (2009).
- [9] M.H. Jamroz, *Vibrational Energy Distribution Analysis; VEDA 4 Program*, Warsaw, Poland (2004).
- [10] M.H. Jamroz, *Spectrochim. Acta A* **114** (2013) 220-230.
- [11] J.P. Merrick, D. Moran, L. Radon, *J. Phys. Chem. A* **111** (2007) 11683-11700.
- [12] M. Silverstein, G. Glayton Basseler, C. Morrill, *Spectrometric Identification of Organic Compounds*, Wiley. New York (1991).
- [13] M. Arirazhagan, J. Senthil Kumar, *Spectrochim. Acta A* **82** (2011) 228.
- [14] V. Arjunan, S. Thillai Govindaraya, P. Ravindran, S. Mohan, *Spectrochim. Acta A* **120** (2014) 473.
- [15] N. Sundaraganesan, S. Ilakiamani, B.D. Joshua, *Spectrochim. Acta A* **467** (2007) 287.
- [16] M. Belletete, J.F. Morin, M. Leclerc, G. Durocher, *J. Phys. Chem. A* **109A** (2005) 6953-6959.
- [17] D. Zhenminga, S. Hepinga, L. Yufanga, L. Diansheng, L. Bob, *Spectrochim. Acta A* **78** (2011) 1143-1148.
- [18] D.F.V. Lewis, C. Loannides, D.V. Parke, *Xenobiotica* **24** (1994) 401.
- [19] E. Scrocco, J. Tomasi, *Adv. Quantum Chem.* **103** (1978) 115-121.
- [20] F.J. Luqul, J.M. Lopez, M. Orozco, *Theor. Chem. Acc.* **103** (2000) 343-345.